RSC Advances

PAPER

View Article Online
View Journal | View Issue

Cite this: *RSC Adv.*, 2021, **11**, 18580

Spent coffee waste as a renewable source for the production of sustainable poly(butylene succinate) biocomposites from a circular economy perspective

Gerda Gaidukova,*[a] Oskars Platnieks,[b] Arturs Aunins,[b] Anda Barkane,[a] Carlo Ingrao[c] and Sergejs Gaidukovs[b]

Received 24th April 2021
Accepted 10th May 2021

DOI: 10.1039/d1ra03203h

rsc.li/rsc-advances

Turning waste products into useable resources is a necessity for the sustainable future of our planet. Such is the case with popular beverage coffee that produces solid waste in the form of spent coffee grounds (SCG). There is an opportunity to use SCG material as a cheap, sustainable, and biodegradable polymer filler that is received as waste from espresso machines. There have been relatively many studies that prove the concept of various agricultural and forestry waste, which can be integrated into modern green materials. Building upon this concept, we have selected a promising polyester poly(butylene succinate) (PBS) as a matrix owing to its bio-based and biodegradable nature. High loadings of SCG from 20 to 60 wt% were tested for optimal composition performance. Tensile, dynamic mechanical, thermal, and structural properties of the composites were examined, while their biodegradation in composting conditions was also analyzed. SCG filler showed different performance from various cellulose fiber-based composites, and properties significantly varied depending on loading. Compared to neat PBS, biodegradation occurred twice as fast for composite materials with high SGC loadings.

1. Introduction

The implementation of bioeconomy and circular economy paradigms in all levels of society is expected to promote national economic growth by saving materials' costs, dampening price volatility, and improving the security of supply chains.[1–3] If on one hand using sustainable ways of treating both raw and secondary resources is very challenging for the industry, on the other hand, it could lead to decreased energy demand for technological manufacturing operations, lower urban waste generation, and the reduced environmental pressures and impacts of industrialization on ecosystems.[4]

Thus, there is an ongoing search for sustainable, cleaner technologies and circular raw materials to fulfill the scarcity of critical resources for the industry's growing demands.[5]

The shift from a linear to a circular model of the economy is increasingly based on achieving and furthering key resource loops such as reuse, repair, remanufacture, and recycling.[2] Furthermore, the efficient collection of waste to be recycled into value-added materials and articles benefiting the national economy, prosperity and environment.[6] Many sustainable technologies, clean fabrication solutions, and circular products are still to be researched and developed.

Coffee and its various beverages have become part of the culture. The coffee beans' annual production in the 2018/2019 crop year exceeded 10 million metric tons, which is almost double compared to 30 years ago.[7] Population growth has resulted in increased demand, leading to various environmental issues from the ineffective use of organic waste and the non-sustainable ways of using limited resources. Therefore, coffee production and consumption clash with different green principles and guidelines, which can be summarized as waste prevention and practical usage.[8]

SCGs produced after the beverages' preparation are almost equal to the initial mass of coffee beans used without including other waste materials produced in the production process.[9] Finding and promoting strategies for waste recirculation within the life cycles of products under the perspective of a circular economy (CE) has become one of the European Union's main goals (EU), to implement and foster sustainable development in the long-term future.[10] CE can play multiple critical roles under this perspective as an invigorating economic model that can help keep materials and products at the top levels of value and utility.[11] The use of landfills should be limited to the most possible to avoid environmental impact sources, like ineffective land use, CO_2 production, the release of caffeine, tannin, and

[a]*Latvian Maritime Academy, Flotes3-7, Riga, LV-1016, Latvia. E-mail: gerda.gaidukova@rtu.lv*

[b]*Faculty of Materials Science and Applied Chemistry, Institute of Polymer Materials, Riga Technical University, P. Valdena 3/7, Riga, LV-1048, Latvia*

[c]*Department of Economics, University of Foggia, Via Romolo Caggese, 1 – 71121 Foggia, Italy*

polyphenols, and other chemicals in the environment.[12–14] Today, it is common to use SCGs as a natural amendment for farming purposes,[15] though it does not allow valorizing SCGs best. Various alternatives have been presented over the years and included the use of SCGs as a direct solid fuel or for the production of biodiesel, biogas, bioethanol, and various extraction products for cosmetics and medicine.[16–20] Other applications like biopolymer synthesis from biowaste and eco-dyeing with SCGs have been proposed.[21–23] Nevertheless, these processes have drawbacks, such as costs, use of toxic chemicals, and mostly lab-based processes that need scaling, while estimates suggest that even centralized processing plants for biodiesel would struggle to compete.[24–26]

SCG composition can vary depending upon the roasting and processing techniques but generally consist of more than 50% carbohydrates that are mainly hemicellulose and cellulose that include their hydrolysis products, while the remaining part comprises lignin, lipids, proteins, minerals, and other substances.[27] Such a composition presents a challenge for complete utilization in the pharmaceutical or biofuel industry, thus preferring the most valuable resources like bio-oils.[28] SCGs are often considered a zero-burden resource that can be transformed into value-added products from a CE perspective. Herein lies the opportunity to use SCGs as filler material for biopolymers to prepare cheap and sustainable biocomposites. Leow proposed to recycle SCGs for useful extracts and green epoxy composites that resulted in materials loaded with up to 30% of SCGs.[29] García-García *et al.* reported the use of 20% of SCG in PP with the use of silanization surface treatment of SCG and a maleated copolymer compatibilizer.[30] Reusing the post-consumer waste espresso coffee capsule waste as raw recycled PP material for the preparation of 30–40% coffee grounds composite is reported recently.[31] Wang used up to 40% of the coffee hull to reinforce polyethylene (PE) matrix composites processed with masterbatch extrusion process.[32]

Several biobased polymers are also considered to obtain SCG composites. Baek[33] explored the filling of polylactic acid (PLA) with SCG and isocyanate-based coupling agents, thereby leading to decreased tensile and flexural strength values to enhance elongation and storage modulus, thus improving ductility. Wu[34] reported PLA/SCG composites disintegration in the composting conditions, and after a two-month period, samples with 20 wt% and 40 wt% loadings of SCGs lost approximately 70% and 90% of their initial weight compared to pure PLA sample that decreased by only 20%. Other studies, like those of García-García *et al.*[30] and Zarrinbakhsh *et al.*[35] examined the application of SCGs as filler for polypropylene (PP) with a 20 to 25 wt% content. They reported that overall mechanical and thermal properties are slightly reduced except for flexural modulus, and even various modification methods did not result in increased properties except for reduced water uptake.[30,35] In another study, Moustafa *et al.*[36] performed a modification of poly(butylene adipate-*co*-terephthalate) (PBAT) with up to 50 wt% SCG. Their study highlighted a significant decrease in mechanical properties, which the authors tried to compensate with the addition of polyethylene glycol (PEG). By doing so, they obtained the composite elongation, but the tensile strength reduced more than two times.[36]

The use of SCGs was found to be beneficial also by Mendes,[37] in the specific case of pectin films. The authors modified those with a 5–20 wt% SCG, and exhibited improved thermal and water vapor barrier properties.[37] Another application field was investigated by Rachtanapun *et al.*[38] who reported thermoset adhesive particleboards using high loadings of SCGs as filler. Research on SCG composites indicates that materials have a high potential for application, but few studies have explored the combination of thermoplastic polymer matrix with high loadings of SCGs.

Previous studies with thermoplastics focused mainly on PLA; thus, we have selected poly(butylene) succinate (PBS) as the matrix. PBS, just like PLA, is a promising bio-based and biodegradable polymer, but the main difference is that at room temperature, it is in the viscoelastic state instead of the glassy state.[39] That provides a critical advantage like relatively large elongation; thus, the structure is more forgiving with highly loaded systems, unlike PLA, which is brittle. PBS has excellent mechanical, thermal properties and is compatible with traditional processing technologies, with the only drawback being relatively low melt strength.[40,41] Research indicates that PBS is applicable and safe for the food-packaging industry and various medical applications.[42,43] Owing to these properties, PBS is seen as a replacement for conventional polymers like polyethylene (PE) and polypropylene (PP).

We have previously demonstrated that recycled cellulose as a cheap and excellent filler can contribute to decreasing economic costs and environmental impacts.[44] Thus, with its high cellulose content, PBS can be a suitable matrix for sustainable, functional composites for a wide range of applications but, mostly, for short life-span plastic products that generate several environmental pollution problems.[45,46]

The ability to make functional wood–plastic composites to avoid usage of natural wood resources could be achieved with SCG, resulting in significantly decreased biodegradation time and reduced cost due to the use of waste products. Omitting the modification methods can simplify production and further decrease costs associated with the usage of bioplastics. While mechanical properties seem to be affected the most, others like barrier properties and thermal properties can be comparable or even enhanced; thus, the preparation of short-life span plastic composites are mutually beneficial.

This paper aims to investigate the use of SCG waste from espresso machines as composite filler to avoid landfill dumping, which is common in Latvia. In this context, the authors have laid a foundation for our research to investigate melt blended PBS/SCG composites for a CE with filler content 20, 40, and 60 wt% to balance the cost and performance aspects. The study reports the findings from experimental research conducted on the lab scale, while a private company provided SCGs. The processed PBS/SCG composites were tested for thermal, tensile, dynamic mechanical, and structural properties and the composting conditions were selected to study the biodegradation.

2. Material and methods

2.1. Material processing

SCGs were received as industrial waste from a company involved in the supply of coffee beans and collection of post-

consumption coffee from restaurants and cafes and mainly consisted of coffee arabica.

Upon arrival at the university lab, SCGs were characterized by a high humidity level; thus, they were dried at room temperature (23 °C, 30% humidity) for five days in large trays. Before being processed into composites, SCGs were ground with a cutting mill (Retsch SM300) to remove agglomerates. Single-stage milling, with manual feeding, 1500 rpm was selected, along with a sieve size of 0.25 mm. BioPBS™ FZ71PB® was purchased from a local supplier, and, according to the producer (PTT MCC Biochem Company Ltd), is declared bio-based (50%), and compatible with conventional industrial applications like thermoplastic extrusion and injection molding. The bio-based mass fraction in this synthetic polymer comes from bio-succinic acid. Succinic acid is a valuable bulk chemical produced from biomass, and further processing can turn it into 1,4-butanediol required for full green synthesis of PBS.[47] Some of the properties provided by the manufacturer include a melting point −115 °C, density −1.36 g cm^{-3}, and melt flow index −22 g/10 min (2.16 kg, 190 °C). The PBS and SCG were dried in a vacuum furnace (J.P. Selecta) at 60 °C for 8 hours before further processing, while heating and the vacuum pump were working periodically to reduce the electricity consumption.

A thermoplastic mixer 50EHT (Brabender®), which is valid to simulate industrial extrusion on the lab scale, was selected for the composite preparation. The processing conditions were adjusted to 70 rpm for twin screws, heating in all zones −130 °C and melt compounding time −7 min.

The experimental study provided the making of a 100%-PBS composite that was used as a reference for comparison with three others made of three different PBS/SCG blends, in which SCGs represented 20, 40, 60 wt% content. The compositions are formulated in Table 1, which examines contributions from bio-based and recycled sources. After melt blending, the samples were grounded using a cutting mill (Retsch SM300, 1500 rpm, 2 mm sieve) to obtain granules for further processing. In the injection molding process (Mini-Jector #55-1E), temperatures were set at:

- 190 °C for the nozzle and front cylinder.
- 185 °C for middle cylinder.
- 180 °C for the rear cylinder.

Dumbbell specimens were obtained from the process and used for tensile testing. After that, testing specimens were cut for density and thermal measurements. While rod-shaped specimens were obtained from the process and used for microscopy. Compression-molded (Carver CH 4386) films of the specimens were prepared with the thickness of 0.10 mm for biodegradation test and 0.20 mm for dynamic mechanical analysis and Vickers microhardness. The compression molding heating plates were set at 190 °C, while the granules were preheated for 2 min, compressed for 3 min (3 MT pressure), cooled for 3 min between steel plates (30 kg of thermal conductive mass).

2.2. Material testing

This section contains a discussion on the testing activities that were carried out on the four PBS/SCG composites obtained as described above to have an overview of the key physical–chemical and mechanical features of the composites in question.

Differential scanning calorimetry. Thermal transitions of the composite materials were studied using DSC-1 (Mettler Toledo). To eliminate the thermal history, the four samples were kept at 150 °C for 5 min after the first heating. The heating and cooling rate were set to 10 °C min^{-1}, while nitrogen was used as a purge gas for all measurements. The crystallinity of PBS and composites were calculated from cooling thermogram data according to eqn (1):[48]

$$\chi_c = \frac{\Delta H_c}{H_m^o(1 - W_{SCG})} \times 100\% \quad (1)$$

where: ΔH_c is the enthalpy of the specimen from the crystallization peak; ΔH_m^o is the theoretical melting enthalpy of 100% crystalline polymer (110.5 J g^{-1} for PBS[49]); and W_{SCG} is the SCG weight content.

Thermogravimetric analysis. Thermogravimetric analysis (TGA) was conducted on a TG50 instrument (Mettler Toledo), following the standard ASTM D3850 procedure, under air atmosphere, and at a heating rate of 10 °C min^{-1}. Samples of a mass of around 10 mg were used.

Hydrostatic density testing. Sartorius KB BA 100 electronic scales equipped with a Sartorius YDK 01 hydrostatic density measurement kit were set up to measure the density (d) in air and ethanol. The density of PBS and the composites was calculated using the following eqn (2):[48]

$$d_p = \frac{m_a(d_{EtOH} - 0.00120)}{0.99983(m_a - m_s)} + 0.00120 \quad (2)$$

where: m_a is the sample's measured mass in air atmosphere; m_s is the sample's measured mass when the sample is submerged in ethanol; d_{EtOH} is the density of ethanol, which was measured with the aerometer.

Vickers microhardness. Vickers M-17 1021 device combined with an optical microscope was set up with 4-time lens magnification, using 0.20 kg indentation load and a 20 s loading time to observe indentations on the surface. The Vickers microhardness of PBS and composites was calculated using the following equation:[44]

Table 1 The prepared PBS/SCG composites and their bio-sourced content

Sample abbreviation	PBS content, wt%	SCG content, wt%	Recycled component, wt%	Bio-based sources, wt%
PBS	100	0	0	50
20%	80	20	20	60
40%	60	40	40	70
60%	40	60	60	80

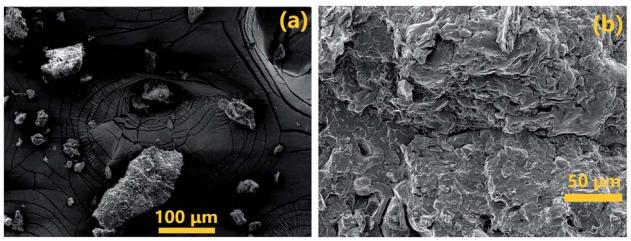

Fig. 1 SEM images: (a) SCG filler and (b) 40 wt% sample.

$$H_V = \sin\left(\frac{\alpha}{2}\right)\frac{Pg}{(dkn/1000)^2} \quad (3)$$

in which: α is the diamond pyramid facet angle (136°); P is the applied load; g is the standard acceleration due to gravity (9.807 m s^{-2} used in our calculations); d is the average diagonal value of the pyramid's indentation; k is the correction factor for the applied load (1.00 from the specification of the instrument for 0.20 kg load); and n is the correction factor for specific lens magnification (1.30 for 4 times magnification).

Dynamic mechanical analysis (DMA). The DMA of the prepared composite samples was performed on the Mettler Toledo DMA/SDTA861e device. All samples were tested in a dual cantilever-measuring system from −80 °C to 80 °C at a heating rate of 3 °C min^{-1} in the air atmosphere with an applied force of 5 N, elongation of 20 μm, frequency of 1 Hz. The sample dimensions were 8.5 × 2 × 0.5 mm.

Scanning electron microscopy. An SEM Tescan Mira\LMU (Czech Republic) microscope was used to obtain images of surface morphology for composite and SCG filler. The composite surface was prepared by a fracture in liquid nitrogen. Images were generated with an acceleration voltage of 5 kV, and the specimens were fixed on standard aluminum pin stubs with an electrically conductive double-sided carbon tape.

Tensile testing. Mechanical properties of the samples were measured by using a universal testing machine Tinius Olsen model 25ST (USA); at least five samples were tested for the tensile properties. The testing machine was equipped with a load cell of 5 kN and tested at 1.0 mm min^{-1} crosshead speed. Samples were dried in a vacuum oven for 8 h at 60 °C and successively preconditioned overnight under the environmental conditions of measurement. Dog-bone shape sample dimensions were 30 × 4 × 2 mm.

Disintegration under composting conditions. The disintegration under composting conditions was carried out using film samples (25 mm × 25 mm × 0.10 mm).[50] Samples were buried at 5 cm depth in plastic boxes containing commercial compost (Kano, Latvia) with a pH value of 5.5 to 7.0. Compost was prepared from Latvian swamp peat with added minerals; (N) 180 mg L^{-1}, (P_2O_5) 245 mg L^{-1}, (K_2O) 400 mg L^{-1}, and Ca, Mg, S, Fe, Mn, Zn, Cu, B, Mo of unspecified content. Aerobic conditions at 58 °C and water humidity at 50% or higher were used for the incubation of 5 specimens for each sample. The recovery of samples was made at every 5 day intervals. After recovery, the samples were washed with distilled water, and a visual appearance was registered before putting them back in the soil.

Melt flow index. The melt flow properties of the samples were measured using a melt flow tester, model MP1200 (Tinus Olsten). The test set up was according to ASTM D1238 standard and carried out at 190 °C with 2.16 kg weight.

3. Results and discussion

3.1. Determination of the structural properties

The SEM images of SCG filler and 40 wt% composites are shown in Fig. 1. SCG particles had a size from few micrometers up to 200 μm and mostly spherical shape, thus indicating particle-based composite instead of fiber-based would be formed. Composite fracture shows a rough surface with some enhanced fractured surface area, but, at the same time, polymer and filler show good melt adhesion. Density test results (Table 2) show an initial increase from 1.22 to 1.30 g cm^{-3} with 20 wt% sample but higher loadings did not follow this trend. In this case, high filler loading could introduce air, agglomerates, and some defects in the structure that result in lower density values.

3.2. Mechanical properties

The tensile modulus, ultimate strength, and elongation at break for the neat PBS and neat PBS/SCG composites have already been shown in Table 2. The addition of relatively high loadings of filler significantly affects material properties, as tensile strength decreased from 31.0 MPa down to 22.6 MPa and 17.8 MPa for 20 and 40 wt% loaded systems, respectively. Such an effect should be attributed to aspects like a potential agglomeration of particles, reduced contact surface with the polymer matrix, and restricted polymer chain movements in line with previous work.[51] Unfortunately, the injection molding device struggled to process 60 wt% loaded composite, mainly because the decrease in melt flow rate was almost 6-fold compared to that in neat PBS. While melt flow rate was only 2-fold lower for 40 wt% loaded composite. This is asserted based upon the melt flow index (MFI) values shown in Table 2.

Table 2 Tensile, surface, melt flow properties and density test results

Sample	MFI, g/10 min (190 °C)	d, g cm^{-3}	HV, MPa	σ, MPa	E, MPa	ε, %
PBS	64 ± 4	1.22 ± 0.04	279 ± 28	31.00 ± 1.60	332 ± 8.5	31.53 ± 3.49
20 wt%	51 ± 1	1.30 ± 0.11	672 ± 25	22.62 ± 1.15	538 ± 24.3	9.27 ± 0.48
40 wt%	38 ± 3	1.28 ± 0.08	741 ± 46	17.84 ± 0.14	619 ± 8.0	4.07 ± 0.27
60 wt%	11 ± 3	1.25 ± 0.14	679 ± 20	7.06 ± 0.45	501 ± 37.9	3.27 ± 0.28

The 60 wt% samples became brittle and had some defects during injection molding. Such a process did not occur, however, for the 20 and 40 wt% loaded samples. Thus, a very low tensile strength value of 7.1 MPa was measured for 60 wt% loadings, and the elastic modulus decreased compared to 20 and 40 wt% loaded samples. The elastic modulus of composites significantly increased from 51 to 86%, consequently, due to the addition of SCGs. An increase of elastic modulus is commonly observed with various cellulose-based materials due to the higher stiffness of these materials than neat polymer. Surface hardness correlates with elastic modulus, thus, composites became more resistant to the abrasion process seen from Vickers microhardness (HV) in Table 2. The addition of SCG resulted in up to a 166% increase compared to neat PBS. The elongation at the break saw a decrease due to the addition of stiffer particles that restricted polymer chain movements. The measured elongation at break 4.07% for 40 wt% and 3.27 wt% are still relatively good values for composites, indicating that they still possess some plasticity. When compared with other bio-based plastics like PLA, which has high glass transition, relatively low elongation due to a glassy state, can provide advantages for using PBS matrix even for highly loaded systems.[52] Leow *et al.* reported a substantial enhancement of the tensile modulus due to increased surface interaction between SCG filler particles and epoxy matrix resin. The observed good homogeneity of the received composites was associated with successful oil removal and refined SCG particles during the coffee extraction process.[29] Authors have also proposed a maleic anhydride coupling agent to facilitate adhesion between polypropylene and coffee grounds, increasing elastic modulus while tensile strength decreased.[31] The reported observation of composites filled with 20% of coffee grounds identified the appearance of stress concentrators as voids and pullouts in fractured tensile surfaces. Other authors report a decrease in the mechanical performances by adding the coffee grounds into the pectin biopolymer due to higher water absorption in humid environments.[53] While it is reported that adding the coffee particles acts as a strong reinforcement for poly(butylene adipate-*co*-terephthalate) and poly(3-hydroxybutyrate-*co*-3-hydroxyvalerate) biopolymer blends.[54]

The storage modulus E', loss modulus E'' and tan δ of neat PBS and SCG composites are shown in parts a to (c) of Fig. 2. As a function of temperature. Storage modulus values showed a sharp decrease in the glass transition region from −20 to +20 °C as commonly observed for polymer materials. SCG filler contributed to the dimensional stability by elevating storage modulus values in the viscous region and showed good interfacial interactions between the filler and matrix. The maximum potential for filler was reached as indicated by similar values of 40 and 60 wt% loadings. The best performance was achieved by the 40 wt% loaded-sample, for which the storage modulus increased in all measured temperature ranges, showing good response on elastic constituent's part. This could be attributed, overall, to 40 wt% samples presenting the best filler dispersion. By contrast, in the 60 wt% loaded sample, the filler severely restricted polymer chain movements and reduced the properties in the glassy state. In case of 20 wt% loading, local agglomerates could significantly reduce the composite properties.

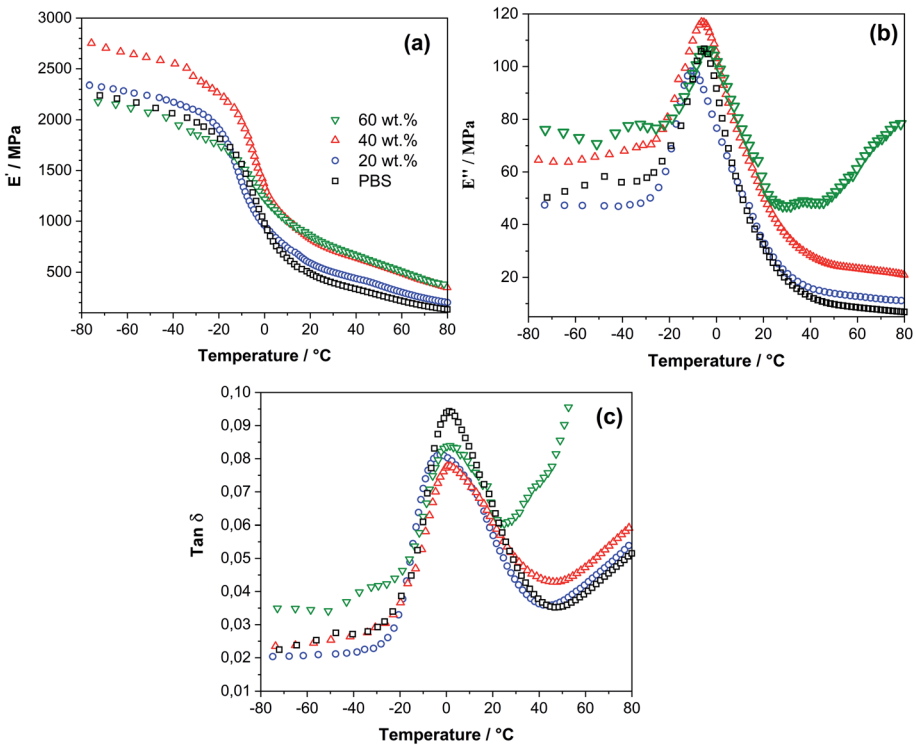

Fig. 2 Temperature dependence of (a) storage modulus, (b) loss modulus, and (c) tan δ curves from DMA measurements comparing PBS and 20, 40, and 60 wt% PBS/SCG composites.

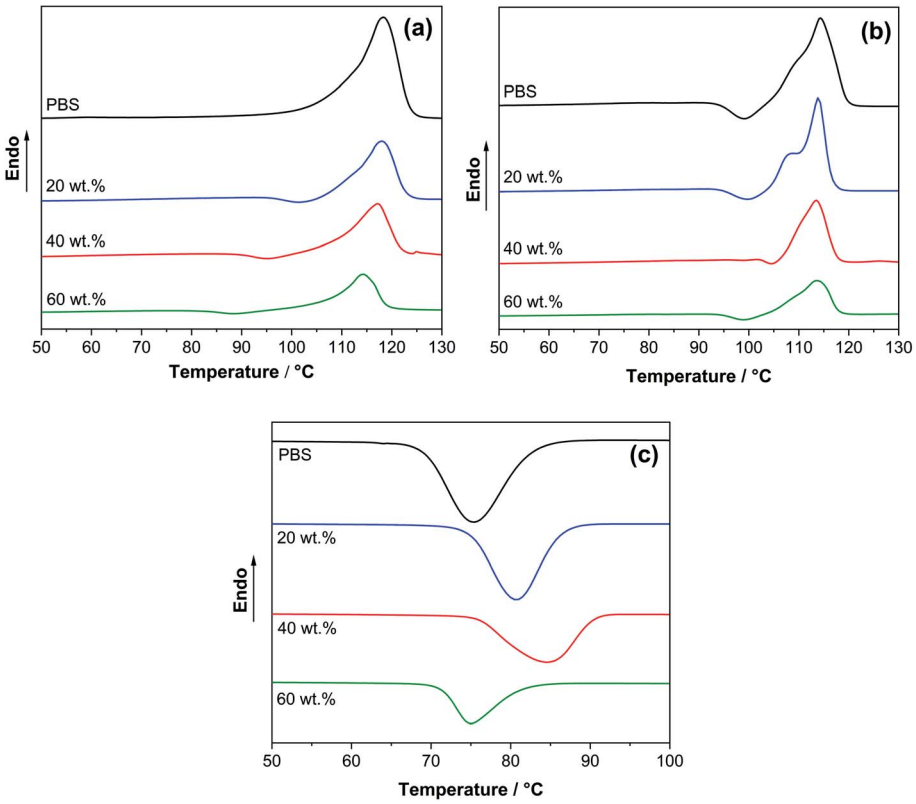

Fig. 3 DSC (a) first heating curves, (b) second heating curves, and (b) cooling curve for PBS and 20, 40, and 60 wt% PBS/SCG composites.

The loss modulus shows a polymeric material and composite ability to dissipate energy and indicates a viscous response of the material, thus stiffness of the material.[55] Polymer composites reinforced with fibers would show decreased loss modulus values owing to their ability to store energy. Only 20 wt% loaded SCG composite showed expected properties with reduced loss modulus values, but only before transitioning into a viscous state. This indicates that SCG did not perform as fiber reinforcement and, instead, worked more as a plasticizer and lubricant. Chang *et al.* reported that loading up to 20% oil extracted SCG into polylactic acid yielded no increase in the stiffness of composite in the viscoelastic state and proposed that the filler acts as a plasticizer.[56] Such results can be beneficial in specific applications and processing techniques like additive manufacturing and injection molding, where material with good melt flow and layer adhesion is required, while high loading is beneficial for a reduced cost. This, in turn, could be the case for SCG due to relatively low cellulose fiber content. As shown in Fig. 2a, the storage modulus steadily increases with SCG particles loading for all frequencies. This increase can be attributed to the rigid nature of the SCG particles, limiting the molecular dynamics of the polymer matrix. The effect of chemical treatment of cellulose grounds and the use of coupling agents could lead to even higher enhancements of the storage and loss modulus values, as discussed in the literature.[57,58]

Damping factor, *i.e.*, the ratio of the loss modulus and storage modulus (E''/E') for the 20 wt% loaded sample remained relatively unchanged compared with neat PBS, except for the decreased value of tan δ peak, indicating that slightly increased interfacial bonding contributed to an overall decrease. 40 and 60 wt% loaded samples saw significantly elevated values in the viscous state due to restricted molecular movements, resulting in the dominance of non-elastic components. The overall high viscous response of 60 wt% sample indicates various structural defects like voids that lead to molecular mobility, and SCG becomes a dominant factor of structural integrity at higher temperatures due to the loss of interfacial bonding.[59] The glass transition temperature remained relatively unchanged with the peak at 1 °C for almost all samples except 20 wt%, which showed a slightly reduced value at −2 °C. Zhang[59] indicated that overall interfacial bonding was relatively weak and made up of intermolecular interactions. At the same time, there was no significant incompatibility observed with the PBS matrix.

3.3. Crystallization and thermal properties

The effect of SCG filler loading on the thermal properties was investigated through calorimetric analysis, and the results are reported in sections a to (c) of Fig. 3. The thermal properties like crystallization temperature (T_c), the first heating melting temperature (T_{m1}), the second heating melting temperature (T_{m2}), crystallization enthalpy (H_c), and crystallinity (χ_c) are reported in Table 3. The DSC first heating scan (Fig. 3a) shows broader melting peaks than the second heating scan (Fig. 3b). This indicates that the cooling process happening in room

Table 3 Thermal properties from DSC and TGA tests

Sample	ΔH_c (J g^{-1})	χ_c (%)	T_c (°C)	T_{m1} (°C)	T_{m2} (°C)	$T_{5\%}$ (°C)	T_{max} (°C)
PBS	73.1	66.2	75.5	118.3	114.4	357	404
20 wt%	58.6	66.3	80.7	118.0	114.0	322	400
40 wt%	47.0	70.9	84.5	117.2	113.5	279	384
60 wt%	26.5	60.0	75.0	114.3	113.5	255	380
SCG	—	—	—	—	—	233	293

temperature injection mold is happing faster than controlled DSC measurement. It has been reported before that PBS crystallizes into primary and secondary lamellar structures, of which one is recrystallizing to perfect form at a temperature close to melting temperature.[60] It is commonly observed for PBS as a broad weak exothermic recrystallization peak just before melting endotherm in thermograms.[61] This shows that rapid cooling creates an unperfect crystalline, *i.e.*, more amorphous, phase, while controlled slow second cooling with DSC results in a more ordered phase that is less susceptible to the heating recrystallization process. With the introduction of SCG, it was possible to understand that it directly interacts with polymer molecules, promoting the nucleation process, and creates a new crystalline phase. The recrystallization exotherm shifts to higher temperature regions. This is seen from higher crystallization temperatures 80 °C for 20 wt% and 85 °C for 40 wt% compared to 75 °C for PBS and change in melting peak shape. While 60 wt% sample showed lower crystallization temperature and crystallinity than PBS; the high loading of SCG significantly restricted the crystallization process. At every loading, different effects of SCG on the PBS crystallization process were observed, where 20 wt% remained closer to PBS, while 40 wt% promoted the crystallization process the most, even achieving higher crystallinity compared to PBS. According to de Bomfim,[31] 30% of coffee filler can decrease the melting enthalpy by 50% and crystallinity by 40% of the polypropylene. The enhancement of the polymer matrix's amorphous phase content after SCG incorporation into the biopolymer was discussed.[62,63]

The thermogravimetric analysis curves of neat PBS, SCG, and composites are shown in Fig. 4. Weight loss after decomposition of 5 wt% ($T_{5\%}$) and the maximum decomposition temperature (T_{max}) are reported in Table 3. Examining components that make up the composite, it is evident that SCG has 111 °C lower maximum decomposition temperature compared to PBS, thus presenting a significant difference in thermal performance. In this case, the polymer matrix would provide shielding for SCG particles inside the composite structure, delaying their decomposition due to relatively low thermal conductivity and providing a reaction with gases in the atmosphere. A good indicator of thermal durability is $T_{5\%}$, which indicates where more significant decomposition starts as small mass losses can occur with loss of low molecular weight molecules, additives, or adsorbed water. The weight content of SCG significantly affects the decomposition temperature for composite materials, as seen from the difference in $T_{5\%}$ values is up to 43 °C between all examined samples. A similar decrease in the thermal stability of composites upon the addition of SCG fillers, as indicated by the earlier onset of decomposition was also reported previously.[29,31] TGA and DTG curves (Fig. 4) showed thermal behavior similar to coffee grounds reported in the literature.[30,57] In the beginning, water evaporation occurs, considering the hydrophilic nature of coffee filler. The subsequent observed weight loss could be associated with the thermal degradation of hemicellulose, followed by cellulose, lignin, and protein thermal decomposition.[30,57] Almost all samples except 60 wt% show single-stage degradation in the derivative mass loss graph. This shows that when filler weight content is higher in composite composition than polymers, the PBS matrix cannot effectively protect SCG from decomposition.

3.4. Compositing performance

It was reported in the literature that one of the main benefits of using SCG or other coffee-based waste products is to accelerate

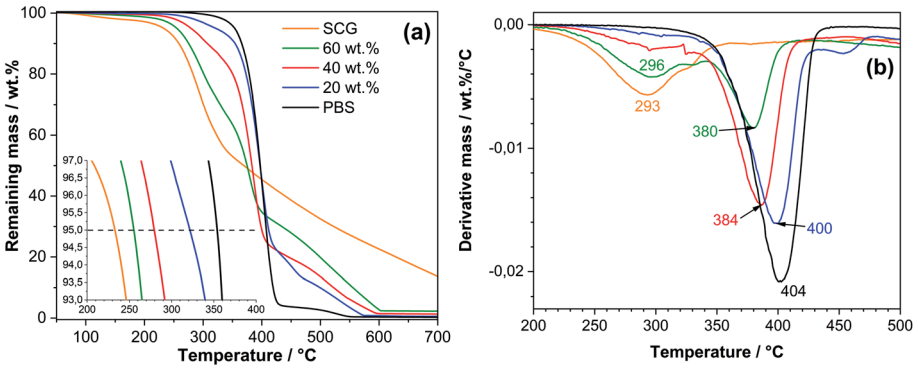

Fig. 4 (a) TGA thermogram and (b) first derivative TGA curves of PBS and PBS/SCG composites.

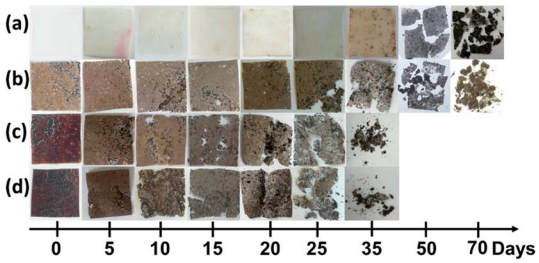

Fig. 5 Photos of (a) PBS; (b) 20 wt%; (c) 40 wt% and (d) 60 wt% films during biodegradation process in the composting conditions.

biodegradation of composite materials made from polyesters like polylactide.[34,64] According to the manufacturer, PBS is compostable in an open-air environment when the temperature is at least 30 °C and does not require industrial composting plants. As discussed before, SCG consists of various molecules that are mainly hydrophilic and thus can attract water molecules and provide the environment for microorganisms. While PBS has a more hydrophobic nature, once the PBS covering layer that protects SCG filler is breached, rapid water adsorption can occur.[65] This can be seen in Fig. 5, where after 5 to 10 days in the soil, composites show signs of degradation compared to pure PBS, which shows slight discoloration on the surface. The highly loaded systems compromised the composite's integrity relatively fast, with 60 wt% becoming fragile and deformed in 10 days, 40 wt% in 15 days, while 20 wt% needed 25 days. PBS and 20 wt% loaded sample degraded from local spots, which then spread to other parts of the composite compared to 40 and 60 wt% samples, which showed a more even disintegration. Thus, PBS and 20 wt% samples needed a significant difference of almost 2-times longer duration. As seen from pictures, agglomerates contributed to much more rapid decomposition observed in 40 and 60 wt% composites.

4. Conclusions

The study attained the proposed goal of exploring the feasibility of using 20–60 wt% SCGs from coffee espresso machines as a zero-burden renewable resource for the preparation of PBS-based composites; relevant findings were obtained. It was, indeed, highlighted that the introduction of SCG to PBS matrices resulted in enhancing their physical–chemical and mechanical properties, though this is in contrast with the currently available literature that showed a decrease in this sense. Such a difference in properties should be attributed to the nature of the polymer material and processing conditions. Experimental results confirmed that SCGs significantly accelerate the biodegradation process in the soil. The mechanical properties for 20 and 40 wt% loaded samples exhibited a decrease in the tensile strength and elongation values but show significantly higher elastic modulus up to 2-fold and Vickers microhardness up to 2.5-fold. The storage modulus increased at higher loadings of 40 and 60 wt%. The highest loaded sample 60 wt% had relatively poor mechanical performance owing to low tensile strength value. Thus, the optimal loading for SCG when mechanical performance was evaluated is 40 wt%. Thermal stability saw a gradual decrease with increased loading of SCG, but samples started decomposition above the processing temperature. All samples showed high crystallinity of 60% or higher, indicating that SCG promotes crystallization and crystalline phase formation in the PBS matrix. The study confirmed that SCGs are composed mainly of hemicellulose, cellulose, lignin, lipids, proteins, and minerals. Their concentration can vary based upon roasting and processing techniques and recycling advancement levels.

This study is part of research aimed at exploring the relevant technical and environmental issues associated with the use of SCGs to produce value-added composites from a CE perspective. The authors propose to expand the research to the environmental life cycle assessment of the SDGs produced and tested in this study.

Author contributions

G. G. contributed to conceptualization; O. P., G. G. contributed to the methodology; A. A. and O. P. contributed to visualization; A. A. contributed to validation; O. P. and G. G. contributed to formal analysis; A. A., O. P., G. G. and A. B. contributed to the investigation; S. G. contributed to resources; O. P. contributed to writing—original draft preparation; O. P., C. I., S. G. and G. G. contributed to writing—review and editing; S. G., C. I., G. G. contributed to supervision. All authors have read and agreed to the published version of the manuscript.

Conflicts of interest

There are no conflicts to declare.

Acknowledgements

The authors wish to thank their parental institutes for providing the necessary facilities to accomplish this work. This work has been supported by the European Regional Development Fund within the Activity 1.1.1.2 “Post-doctoral Research Aid” of the Specific Aid Objective 1.1.1 “To increase the research and innovative capacity of scientific institutions of Latvia and the ability to attract external financing, investing in human resources and infrastructure” of the Operational Programme “Growth and Employment” (No. 1.1.1.2/VIAA/3/19/478).

Notes and references

1 Y. Kalmykova, M. Sadagopan and L. Rosado, *Resour., Conserv. Recycl.*, 2018, **135**, 190–201.
2 C. Ingrao, C. Arcidiacono, V. Siracusa, M. Niero and M. Traverso, *Resources*, 2021, **10**, 32.
3 C. Ingrao, J. Bacenetti, A. Bezama, V. Blok, P. Goglio, E. G. Koukios, M. Lindner, T. Nemecek, V. Siracusa, A. Zabaniotou and D. Huisingh, *J. Cleaner Prod.*, 2018, **204**, 471–488.
4 G. Y. Piergiuseppe Morone, *Acta Innovations*, 2020, 5–16, DOI: 10.32933/ActaInnovations.36.1.

5 T. R. Burns, *Sustainability*, 2012, **4**, 6.
6 M. S. Andersen, *Sustainability Science*, 2007, **2**, 133–140.
7 ICO, International Coffee Organization, http://www.ico.org/historical/1990%20onwards/PDF/1a-total-production.pdf, accessed 25.09.2020.
8 D. Lenoir, K.-W. Schramm and J. O. Lalah, *Sustainable Chem. Pharm.*, 2020, **18**, 100313.
9 L. Blinová, M. Sirotiak, A. Bartošová and M. Soldán, *Res. Pap. - Fac. Mater. Sci. Technol., Slovak Univ. Technol.*, 2017, **25**, 91–101.
10 *A new Circular Economy Action Plan For a cleaner and more competitive Europe*, https://eur-lex.europa.eu/legal-content/EN/TXT/?qid=1583933814386&uri=COM:2020:98:FIN, accessed 12.12.2020.
11 C. Ingrao, N. Faccilongo, L. Di Gioia and A. Messineo, *J. Cleaner Prod.*, 2018, **184**, 869–892.
12 J. Kim, H. Kim, G. Baek and C. Lee, *Waste Manag.*, 2017, **60**, 322–328.
13 S. I. Mussatto, E. M. S. Machado, S. Martins and J. A. Teixeira, *Food Bioprocess Technol.*, 2011, **4**, 661–672.
14 J. P. Bok, H. S. Choi, Y. S. Choi, H. C. Park and S. J. Kim, *Energy*, 2012, **47**, 17–24.
15 C. K. Morikawa and M. Saigusa, *Plant Soil*, 2008, **304**, 249–255.
16 S. K. Karmee, *Waste Manag.*, 2018, **72**, 240–254.
17 P.-T. Yeung, P.-Y. Chung, H.-C. Tsang, J. Cheuk-On Tang, G. Yin-Ming Cheng, R. Gambari, C.-H. Chui and K.-H. Lam, *RSC Adv.*, 2014, **4**, 38839–38847.
18 N. Ramirez, F. Sardella, C. Deiana, A. Schlosser, D. Müller, P. A. Kißling, L. F. Klepzig and N. C. Bigall, *RSC Adv.*, 2020, **10**, 38097–38106.
19 S. M. Unni, L. George, S. N. Bhange, R. N. Devi and S. Kurungot, *RSC Adv.*, 2016, **6**, 82103–82111.
20 B. Sukhbaatar, B. Yoo and J.-H. Lim, *RSC Adv.*, 2021, **11**, 5118–5127.
21 I. S. Fahim, H. Chbib and H. M. Mahmoud, *Sustainable Chem. Pharm.*, 2019, **12**, 100142.
22 R. Mongkholrattanasit, M. Nakpathom and N. Vuthiganond, *Sustainable Chem. Pharm.*, 2021, **20**, 100389.
23 S. M. K. Thiagamani, R. Nagarajan, M. Jawaid, V. Anumakonda and S. Siengchin, *Waste Manag.*, 2017, **69**, 445–454.
24 D. S. Scully, A. K. Jaiswal and N. Abu-Ghannam, *Bioengineering*, 2016, **3**, 33.
25 I. K. Kookos, *Resour., Conserv. Recycl.*, 2018, **134**, 156–164.
26 N. Tuntiwiwattanapun, P. Usapein and C. Tongcumpou, *Energy Sustainable Dev.*, 2017, **40**, 50–58.
27 T. M. Mata, A. A. Martins and N. S. Caetano, *Bioresour. Technol.*, 2018, **247**, 1077–1084.
28 J. Rajesh Banu, S. Kavitha, R. Yukesh Kannah, M. Dinesh Kumar, A. Preethi, A. E. Atabani and G. Kumar, *Bioresour. Technol.*, 2020, **302**, 122821.
29 Y. Leow, P. Y. M. Yew, P. L. Chee, X. J. Loh and D. Kai, *RSC Adv.*, 2021, **11**, 2682–2692.
30 D. García-García, A. Carbonell, M. D. Samper, D. García-Sanoguera and R. Balart, *Composites, Part B*, 2015, **78**, 256–265.
31 A. S. Campos de Bomfim, H. J. Cornelis Voorwald, K. C. Coelho de Carvalho Benini, D. Magalhães de Oliveira, M. F. Fernandes and M. O. Hilário Cioffi, *J. Cleaner Prod.*, 2021, **297**, 126647.
32 Z. Wang, L. Dadi Bekele, Y. Qiu, Y. Dai, S. Zhu, S. Sarsaiya and J. Chen, *Bioengineered*, 2019, **10**, 397–408.
33 B. S. Baek, J. W. Park, B. H. Lee and H. J. Kim, *J. Polym. Environ.*, 2013, **21**, 702–709.
34 C.-S. Wu, *Polym. Degrad. Stab.*, 2015, **121**, 51–59.
35 N. Zarrinbakhsh, T. Wang, A. Rodriguez-Uribe, M. Misra and A. K. Mohanty, *Bioresources*, 2016, **11**, 7637–7653.
36 H. Moustafa, C. Guizani and A. Dufresne, *J. Appl. Polym. Sci.*, 2017, **134**, 44498.
37 J. F. Mendes, J. T. Martins, A. Manrich, A. R. Sena Neto, A. C. M. Pinheiro, L. H. C. Mattoso and M. A. Martins, *Carbohydr. Polym.*, 2019, **210**, 92–99.
38 P. Rachtanapun, T. Sattayarak and N. Ketsamak, *J. Compos. Mater.*, 2012, **46**, 1839–1850.
39 J.-x. Qin, M. Zhang, C. Zhang, C.-t. Li, Y. Zhang, J. Song, H. M. Asif Javed and J.-h. Qiu, *RSC Adv.*, 2016, **6**, 17896–17905.
40 M. Zhang, Y. Li, L. Wang and S. Li, *J. Appl. Polym. Sci.*, 2019, **137**, 48740.
41 B. A. Calderón, J. Soule and M. J. Sobkowicz, *J. Appl. Polym. Sci.*, 2019, **136**, 47553.
42 S. Vytejčková, L. Vápenka, J. Hradecký, J. Dobiáš, J. Hajšlová, C. Loriot, L. Vannini and J. Poustka, *Polym. Test.*, 2017, **60**, 357–364.
43 M. Gigli, M. Fabbri, N. Lotti, R. Gamberini, B. Rimini and A. Munari, *Eur. Polym. J.*, 2016, **75**, 431–460.
44 O. Platnieks, A. Barkane, N. Ijudina, G. Gaidukova, V. K. Thakur and S. Gaidukovs, *J. Cleaner Prod.*, 2020, **270**, 122321.
45 C. J. Rhodes, *Sci. Prog.*, 2019, **101**, 207–260.
46 K. Jõgi and R. Bhat, *Sustainable Chem. Pharm.*, 2020, **18**, 100326.
47 J. Lu, J. Li, H. Gao, D. Zhou, H. Xu, Y. Cong, W. Zhang, F. Xin and M. Jiang, *World J. Microbiol. Biotechnol.*, 2021, **37**, 16.
48 S. Gaidukov, U. Cabulis, K. Gromilova, V. Tupureina and A. Grigalovica, *Int. J. Polym. Sci.*, 2013, **2013**, 1–8.
49 M. S. Nikolic and J. Djonlagic, *Polym. Degrad. Stab.*, 2001, **74**, 263–270.
50 O. Platnieks, S. Gaidukovs, A. Barkane, A. Sereda, G. Gaidukova, L. Grase, V. K. Thakur, I. Filipova, V. Fridrihsone, M. Skute and M. Laka, *Polymers*, 2020, **12**, 1–20.
51 S. Chuayjuljit, C. Wongwaiwattanakul, P. Chaiwutthinan and P. Prasassarakich, *Polym. Compos.*, 2017, **38**, 2841–2851.
52 S. Su, R. Kopitzky, S. Tolga and S. Kabasci, *Polymers*, 2019, **11**, 1193.
53 V. A. Cataldo, G. Cavallaro, G. Lazzara, S. Milioto and F. Parisi, *Carbohydr. Polym.*, 2017, **170**, 198–205.
54 F. Sarasini, J. Tirillò, A. Zuorro, G. Maffei, R. Lavecchia, D. Puglia, F. Dominici, F. Luzi, T. Valente and L. Torre, *Ind. Crops Prod.*, 2018, **118**, 311–320.
55 F. Ahmad, N. Yuvaraj and P. K. Bajpai, *Compos. Struct.*, 2021, **255**, 112955.

56 Y.-C. Chang, Y. Chen, J. Ning, C. Hao, M. Rock, M. Amer, S. Feng, M. Falahati, L.-J. Wang, R. K. Chen, J. Zhang, J.-L. Ding and L. Li, *ACS Sustainable Chem. Eng.*, 2019, **7**, 15304–15310.
57 H. Essabir, M. Raji, S. A. Laaziz, D. Rodrique, R. Bouhfid and A. e. k. Qaiss, *Composites, Part B*, 2018, **149**, 1–11.
58 A. Nanni and M. Messori, *J. Appl. Polym. Sci.*, 2020, **137**, 48869.
59 Z. Zhang, P. Wang and J. Wu, *Phys. Procedia*, 2012, **25**, 305–310.
60 G. Z. Papageorgiou, D. S. Achilias and D. N. Bikiaris, *Macromol. Chem. Phys.*, 2007, **208**, 1250–1264.
61 Y. J. Phua, N. S. Lau, K. Sudesh, W. S. Chow and Z. A. Mohd Ishak, *Polym. Degrad. Stab.*, 2012, **97**, 1345–1354.
62 S. M. Kumar, K. Yorseng, A. Nadir, S. Siengchin, N. Ayrilmis and V. Rajulu, *Process Saf. Environ. Prot.*, 2019, **124**, 187–195.
63 V. A. Yiga, S. Pagel, M. Lubwama, S. Epple, P. W. Olupot and C. Bonten, *J. Thermoplast. Compos. Mater.*, 2019, **33**, 1269–1291.
64 A. P. da Silva, M. d. P. Pereira, F. R. Passador and L. S. Montagna, *Macromol. Symp.*, 2020, **394**, 2000091.
65 O. Platnieks, S. Gaidukovs, A. Barkane, G. Gaidukova, L. Grase, V. K. Thakur, I. Filipova, V. Fridrihsone, M. Skute and M. Laka, *Molecules*, 2020, **25**, 121.